Performance of the ALICE VZERO system

2013 JINST 8 P10016

(http://iopscience.iop.org/1748-0221/8/10/P10016)

PUBLISHED BY IOP PUBLISHING FOR SISSA MEDIALAB

RECEIVED: *June 13, 2013*
ACCEPTED: *September 18, 2013*
PUBLISHED: *October 14, 2013*

Performance of the ALICE VZERO system

The ALICE collaboration

E-mail: ALICE-publications@cern.ch

ABSTRACT: ALICE is an LHC experiment devoted to the study of strongly interacting matter in proton-proton, proton-nucleus and nucleus-nucleus collisions at ultra-relativistic energies. The ALICE VZERO system, made of two scintillator arrays at asymmetric positions, one on each side of the interaction point, plays a central role in ALICE. In addition to its core function as a trigger source, the VZERO system is used to monitor LHC beam conditions, to reject beam-induced backgrounds and to measure basic physics quantities such as luminosity, particle multiplicity, centrality and event plane direction in nucleus-nucleus collisions. After describing the VZERO system, this publication presents its performance over more than four years of operation at the LHC.

KEYWORDS: Large detector-systems performance; Trigger detectors; Large detector systems for particle and astroparticle physics; Heavy-ion detectors

doi:10.1088/1748-0221/8/10/P10016

Contents

2013 JINST 8 P10016

1 Introduction

ALICE (A Large Ion Collider Experiment) is an experiment dedicated to the study of heavy-ion collisions at the LHC [1, 2]. It is designed to explore the physics of strongly interacting matter in proton-proton (pp) collisions and of Quark-Gluon Plasma (QGP) at extreme values of energy density and temperature in nucleus-nucleus collisions. It provides identification of particles up to the highest multiplicities and down to low transverse momentum ($p_{\mathrm{T}} \gtrsim 50\,\mathrm{MeV}/c$). The physics programme also includes proton-nucleus collisions in order to study the cold nuclear effects, and lighter ion collisions in order to vary energy density and interaction volume. Data taking in pp mode provides reference data for the heavy-ion programme and allows to investigate various specific properties of the strong-interaction, thereby playing a complementary role to that of the other LHC experiments.

The ALICE apparatus consists of a central barrel, a forward muon spectrometer and a set of detectors in the forward regions including the VZERO system. This system provides triggers for the experiment (minimum bias or centrality trigger) and separates beam-beam interactions from background events such as beam-gas interactions, either at trigger level or in off-line analyses. Furthermore, it is also used to measure beam luminosity, charged particle multiplicity and azimuthal distributions. The control of the luminosity allows the determination of the absolute cross-section value of reaction processes. The knowledge of the charged particle multiplicity is essential for the evaluation of the centrality of nucleus-nucleus collisions. The particle azimuthal distribution is important for determining the Pb-Pb collision reaction plane.

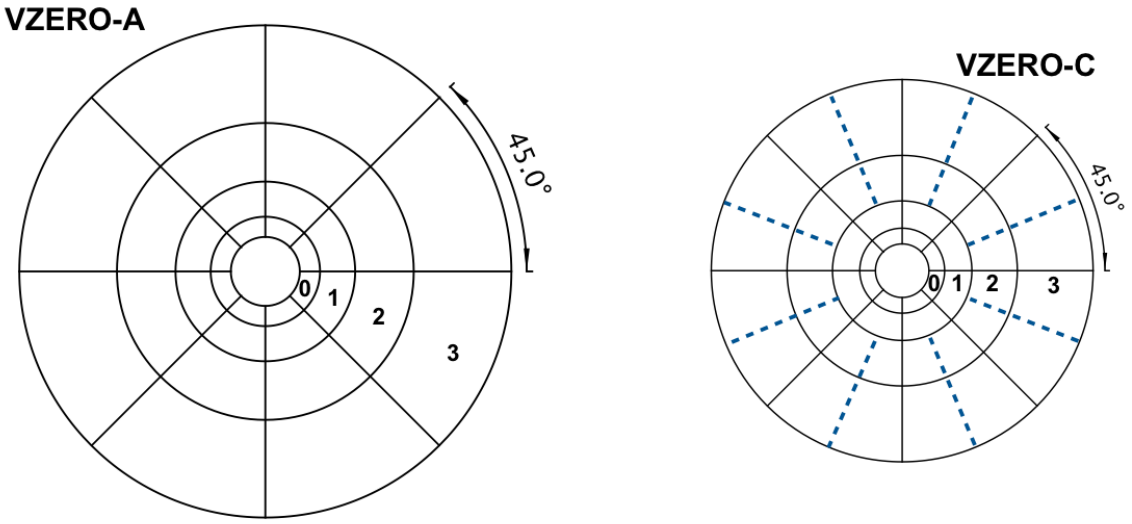

Figure 1. Sketches of VZERO-A and VZERO-C arrays showing their segmentation. Scintillator thicknesses are 2.5 and 2 cm respectively. Radii of rings are given in table 1. The scintillator segments on both sides of the dashed lines are connected to the same PMT (see section 3).

In this publication, a description of the VZERO system and its Front-End Electronics (section 2) is given as well as the calibration procedure for individual channels (section 3). Details about the role of the system in the ALICE triggering scheme (section 4) are then described. Finally, its use for physics purposes, is also pointed out: monitoring of colliding beams for the evaluation of luminosity (section 5); measurement of the multiplicity for the estimation of the centrality of collisions (section 6); measurement of azimuthal distributions of charged particles for the knowledge of the anisotropic flow of collisions (section 7). The last three sections are only briefly covered, since detailed developments have already been published.

2 The VZERO system

The detailed description of the VZERO system may be found in [3, 4] and references therein. It is composed of two arrays, VZERO-A and VZERO-C, which cover the pseudorapidity ranges $2.8 < \eta < 5.1$ and $-3.7 < \eta < -1.7$ for collisions at the nominal vertex ($z = 0$). Each of the VZERO arrays is segmented in four rings in the radial direction, and each ring is divided in eight sections in the azimuthal direction (figure 1). The pseudorapidity coverage of each ring is given in table 1. Each channel of both arrays is made of a BC404 plastic scintillator from Bicron [5] with a thickness of 2.5 and 2.0 cm for VZERO-A and VZERO-C respectively. BCF9929A Wave-Length Shifting (WLS) fibers from Bicron are embedded in both faces of the segments (VZERO-A) or glued along their two radial edges (VZERO-C). Figure 2 shows a schematic view of an elementary cell of each array. These two different designs were mandatory to comply with the integration constraints of each array. The VZERO-A is located 329 cm from the nominal vertex ($z = 0$) on the side opposite to the muon spectrometer (figure 3). The VZERO-C is fixed on the front face of the hadronic absorber. The position of the various rings of the VZERO-C along the z direction

2013 JINST 8 P10016

Table 1. Pseudorapidity and angular (deg.) acceptances, radius coverage (cm) and z (cm) position along the beam axis of VZERO-A and VZERO-C median plane rings, as seen from the origin of the coordinate system.

Ring	VZERO-A				VZERO-C			
	η_{max}/η_{min}	$\theta_{min}/\theta_{max}$	r_{min}/r_{max}	z	η_{min}/η_{max}	$\theta_{max}/\theta_{min}$	r_{min}/r_{max}	z
0	5.1/4.5	0.7/1.3	4.3/7.5	329	-3.7/-3.2	177.0/175.3	4.5/7.1	-86
1	4.5/3.9	1.3/2.3	7.7/13.7	329	-3.2/-2.7	175.3/172.3	7.3/11.7	-87
2	3.9/3.4	2.3/3.8	13.9/22.6	329	-2.7/-2.2	172.3/167.6	11.9/19.3	-88
3	3.4/2.8	3.8/6.9	22.8/41.2	329	-2.2/-1.7	167.6/160.0	19.5/32.0	-88

is given in table 1. The specific geometry of the VZERO-C array permits an optimized azimuthal coverage while leaving room for the passage of the WLS fibers. As shown in figure 2 there are no such constraints for the VZERO-A array.

The light is transferred to the R5946-70 photomultiplier tube (PMT) (Hamamatsu [6]) directly for VZERO-A and through an extra 3 m of PMMA (Poly(methyl methacrylate)) clear fibers (Mitsubishi [7]) for VZERO-C (figure 2). Fine mesh PMTs were chosen for their capacity to operate in a magnetic field, since the VZERO arrays and their PMTs are inside the ALICE solenoid which produces a field of 0.5 T. In order to minimize the signal attenuation, the tube axis are oriented at 30° relatively to the magnetic field direction. For the two outer rings of the VZERO-C array, each sector is divided into two segments of 22.5° (figure 1) both connected to the same PMT. This separation was necessary to optimize the light collection by the WLS fibers glued on the radial edges of the segments.

For each elementary cell, the PMT output is split into two signals sent to the Front-End Electronics (FEE), one of them after amplification by a factor 10. For the 32 channels of each array [8], the pulse time (leading time) relative to the 40 MHz LHC bunch clock and the width at discriminator threshold are measured by time to digital converters (TDC) on amplified signals, and the charge is integrated by charge analog to digital converters (ADC) on direct signals. Two types of trigger algorithms are implemented independently for VZERO-A and VZERO-C arrays. The first trigger type is based on pre-adjusted time windows corresponding to beam-beam or beam-background in coincidence with the time signals from the counters. It is used to select minimum bias events and to reject beam-induced background events. The second trigger type is based on the total charge collected by each array. Pb-Pb collisions corresponding to centralities 0–10% to 0–50% can then be selected. Finally, five trigger sources [8], chosen according to specific features of collision mode and recorded data, are sent to the Central Trigger Processor (CTP) [9]. The CTP collects signals from all trigger devices, provides trigger decisions and distributes global trigger signals to the whole ALICE experiment, together with the LHC clock and timing synchronization information. ALICE has a multi-level trigger protocol named L0, L1 and L2, with latency with respect to the collision time of 1.2, 6.5 and 88 μs, respectively. The VZERO arrays contribute to the L0 trigger decision.

2013 JINST 8 P10016

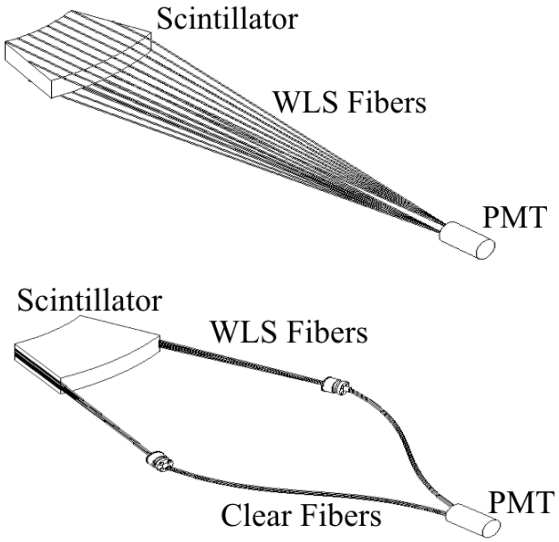

Figure 2. Schematic drawings of elementary cell designs for VZERO-A (top) and VZERO-C rings 0-1 (bottom). For VZERO-C rings 2-3, two scintillating sets (scintillator and WLS fibers) are connected to a single PMT through four clear fiber beams (see figure 1).

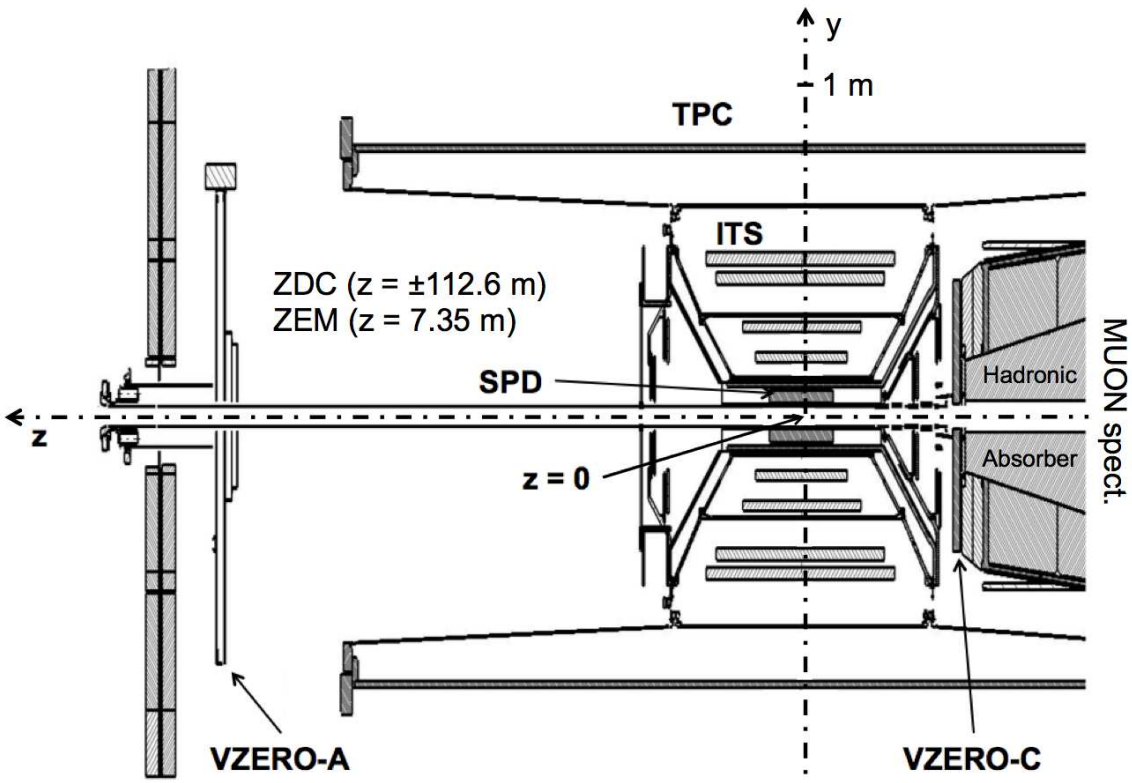

Figure 3. Position of the two VZERO arrays, and of the few detectors quoted in the text, within the general layout of the ALICE experiment.

2013 JINST 8 P10016

3 Detector calibrations and data corrections

For each channel, two quantities need to be calibrated to ensure uniform output for all the channels of the detector: the PMT gain and the light yield of the scintillator-fibers assembly. The latter takes into account both the light yield of the scintillator elements and the light transmission through the WLS fibers and optical fiber lines. The calibration of the detector was carried out in two steps. The gain curve of each PMT was determined in the laboratory using cosmic muons passing through a scintillator cell. Measurements at three high voltages were carried out. The high charge resolution of the XP2020 PMT (Photonis [10]) calibrated with a LED source, made it possible to measure the average number of photo-electrons produced in the VZERO scintillators, thus providing an absolute gain measurement of VZERO PMTs. The light yield of each optical line was measured in situ with pp collisions at $\sqrt{s} = 7\,\text{TeV}$. Using a simulation of the detector and knowing the gain vs. high voltage curve of each PMT, it was possible to determine the light yields of individual channels. The high voltage of each channel was then adjusted to have the same response to the passage of one minimum ionizing particle (MIP) in terms of ADC counts (about 15 ADC counts per MIP in pp collision mode). The resulting amplitude distributions are uniform within 10–20% (figure 4-top). The average high voltage in pp collision mode is around 2000 V. To cope with the large charged particle multiplicity in Pb-Pb collisions without saturating the ADCs, the voltages are reduced to about 1500 V, corresponding to a reduction factor of about 10 for the PMTs gains in comparison with pp voltages.

Relative time adjustment between channels was done using a cable with a length known with a precision of 1 ns. Fine tuning adjustment was performed using individual programmable delays on the FEE boards, resulting in a uniform response of the elementary cells (figure 4-bottom). The time of flight of particles coming from the Interaction Point (IP) to the VZERO-A (VZERO-C) is about 11 ns (3 ns). The dashed line in figure 4-bottom represents the collision time. For beam induced background coming from the C side (A side) to the VZERO-A (VZERO-C) the time of flight is also 11 ns (3 ns). Furthermore, a signal arriving at -11 ns (-3 ns) to the VZERO-A (VZERO-C) can be clearly seen. It corresponds to particles from beam induced background coming from the A side (C side). In this case, the dashed line represents the time when particles cross the vertical plane at $z = 0$.

Due to the fact that threshold discriminators are used, the leading time measurement is affected by a slewing effect. Then, the measured time of the rising signal depends on its amplitude as shown in figure 5-left. The measured raw time t_{raw} is corrected for slewing effect by subtracting an offset $\Delta t(Q)$, function of the pulse charge Q: $t_{\text{corr}} = t_{\text{raw}} - \Delta t(Q)$. The offset calculation uses the following parametrization:

$$\Delta t(Q) = C\sqrt{\frac{s}{Q}}, \tag{3.1}$$

where C is a constant equal to 10.5 ns and s the threshold setting of the discriminator fixed to 1 (4) ADC channel(s) for Pb-Pb (pp) collisions.

The effect of this correction is shown in figure 5-right. The average time response is then independent of the charge delivered by the PMT. The time resolution dependence on the signal can be deduced from this plot. Averaged over all signal amplitudes, the individual channel time

2013 JINST 8 P10016

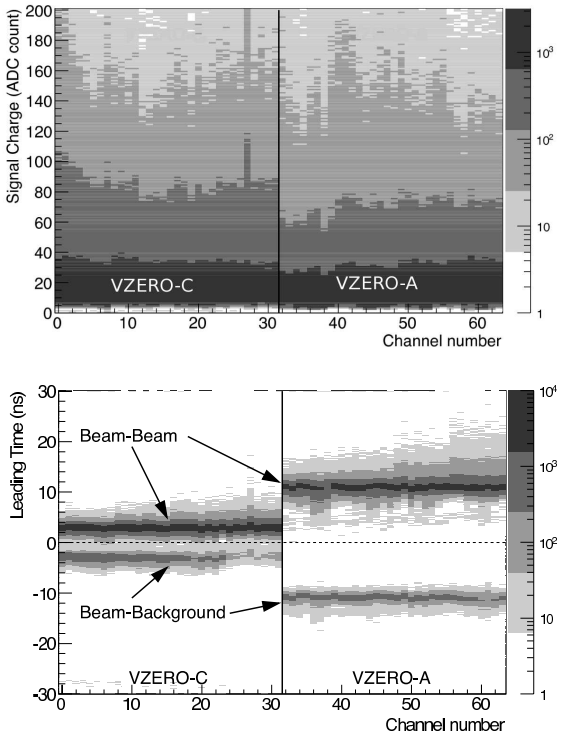

Figure 4. Charge of the pulse in ADC counts (top) and leading time of the pulse in nanoseconds (bottom) versus channel number for pp collisions at $\sqrt{s} = 7\,\text{TeV}$. Channels numbered from 0 to 31 correspond to VZERO-C, channels numbered from 32 to 63 correspond to VZERO-A.

resolution is of the order of 1 ns for both arrays. This time resolution is independent of the colliding system (pp or Pb-Pb).

Since 2009, the VZERO detector has been exposed to radiation produced by the LHC. Both beam-beam collisions and beam-induced backgrounds contribute to the accumulated radiation dose. We observed a loss in signal amplitude of 10 to 40% at the end of 2012, depending on the channel, which is attributed to ageing effect. An accurate determination of the accumulated dose is difficult due to uncertainties in the beam-induced background evaluation. Nevertheless, from the luminosity measurement and the background monitoring, we can estimate that the total accumulated dose per channel does not exceed 50 krad. This value is six times lower than the maximum dose accumulated during a radiation tolerance test using a 60 MeV proton beam [11]. Results from this test show that the loss of signal from the scintillating material is in the order of a few percent at 50 krad, which cannot explain the observed reduction of signal amplitude. The dominant contribution to the loss is attributed to ageing of the PMT photocathodes. This effect was shown by monitoring the signal amplitude from direct particle hits on the PMT compared to the signal amplitude from scintillation, the discrimination between both components being possible as the timing difference between these two sources is around 6 ns for the VZERO-A side and even longer for the VZERO-C side. Early 2013, after the LHC shutdown, a set of 6 PMT chosen randomly were extracted from the experiment to be tested in laboratory. For each of them, the gain measured in 2013 and compared to the one measured in 2006 before the installation, shows the same loss

2013 JINST 8 P10016

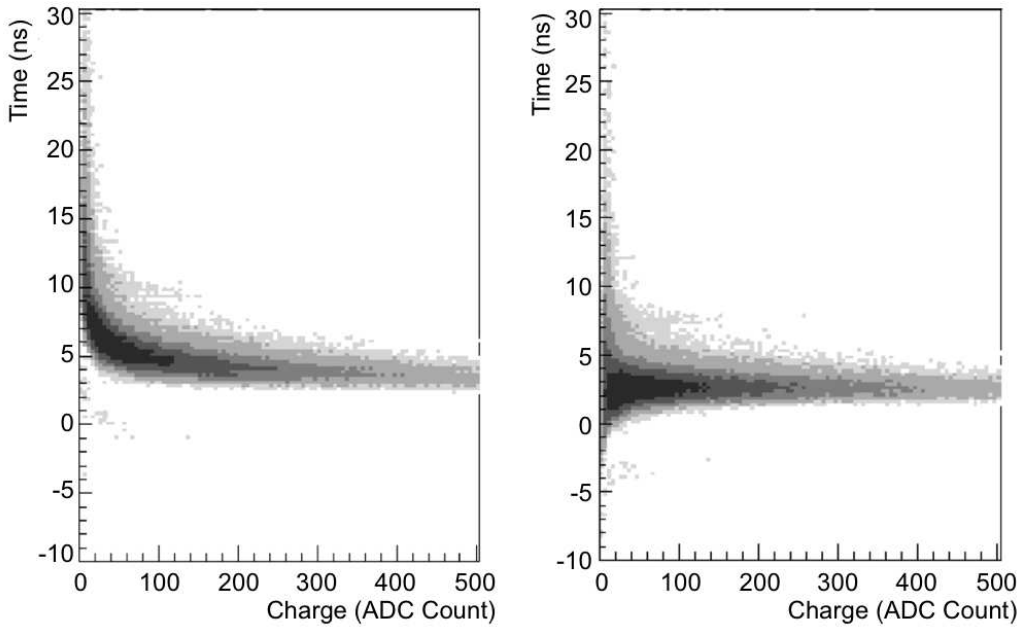

Figure 5. Correlation between leading time in nanoseconds and charge of the PMT signals in ADC channel counts for Pb-Pb collisions, before any correction (left) and after slewing correction (right).

than the one measured in the experiment. To compensate for the signal loss and adjust the gain approximately at its initial value, the individual PMT high voltage had to be increased accordingly.

4 The VZERO trigger system

One of the primary roles of the VZERO system is to provide the ALICE experiment with a minimum bias (MB) trigger both in pp and Pb-Pb collisions and with centrality based triggers in Pb-Pb mode. The VZERO system has been operational throughout the whole period of ALICE operating since 2009, thus demonstrating the stability and robustness of the detector and its readout system.

In the 2009 and 2010 pp data taking periods, the ALICE MB trigger MB_{OR} was built requiring a hit in the Silicon Pixel Detector (SPD in figure 3) which is the innermost part of the Inner Tracking System (ITS) [4] or in either of the VZERO arrays (VZERO-A or VZERO-C). The threshold setting of the VZERO individual channels corresponds approximately to one quarter of the mean energy deposit by a minimum ionizing particle. This MB trigger was set in coincidence with signals from two beam pick-up counters, one on each side of the interaction region, indicating the passage of proton bunches. This trigger corresponds to the requirement of at least one charged particle anywhere in 8 units of pseudorapidity. During the 2011 and 2012 pp data taking periods, with the increasing LHC luminosity and beam background, the trigger moved to a stricter condition using the coincidence either between both VZERO arrays and the LHC bunch crossing signals, or between both VZERO arrays, the LHC bunch crossing signals and any other detector triggering on specific event topology like the muon spectrometer or the electromagnetic calorimeter. The last configuration was used to search for rare physics signals.

2013 JINST 8 P10016

In Pb-Pb collisions, the interaction trigger is configured to obtain high efficiency for hadronic interactions, requiring at least two out of the following three conditions: (i) two pixel chips hit in the outer layer of the SPD, (ii) a signal in VZERO-A, (iii) a signal in VZERO-C. The threshold setting corresponds approximately to the mean energy deposited by one minimum ionizing particle. The PMT gains are reduced by a factor of 10 in order not to saturate the ADC for the most central collisions. At the end of the 2010 Pb-Pb data taking period, as the beam luminosity increased, the minimum bias trigger had to be restricted to the coincidence between SPD, VZERO-A and VZERO-C in order to suppress signals created by electromagnetic dissociation of Pb nuclei as much as possible. During the full 2011 Pb-Pb run, the VZERO delivered three different triggers: (i) the VZERO-A and VZERO-C coincidence asking for at least one cell hit in each array, (ii) a trigger signal selecting the collisions corresponding to a centrality of 0–50%, (iii) a trigger signal selecting the 0–10% most central collisions (see figure 8).

In both running modes (pp and Pb-Pb), a non-negligible background comes from interactions between the beams and the residual gas within the beam pipe and from interactions between the beam halo and various components of the accelerator such as collimators. Using the time of flight of particles detected by each VZERO array, particles coming from collisions and particles coming from beam-gas background can be clearly distinguished.

Two beam-gas background selections can be applied thanks to the VZERO system, one on-line at the FEE level and one off-line at the data reconstruction stage. In the FEE, coincidence windows of 8 ns in length are placed around the beam-beam timing in order to select the beam-beam events and reject most of the beam-induced background events. It increases the fraction of good events recorded in the data. This information is also used in order to monitor the level of beam induced background. This selection was in production starting with the 2012 run due to the increase of luminosity and beam-induced background level.

The second selection, performed off-line, is more refined. For each VZERO array, a weighted average time of flight over the channels above threshold is calculated. As shown in figure 5-right, the time measurement resolution is better for larger amplitude signals. Therefore, for each channel hit, a weight function $\omega(Q) = 1/\sigma^2(Q)$ is calculated where $\sigma(Q)$ is the channel time resolution parametrized as:

$$\sigma(Q) = \sqrt{a^2 + \frac{b^2}{N_e} + c^2 \frac{s}{Q^3}}, \tag{4.1}$$

where N_e is the mean number of photo-electrons obtained from the pulse charge and the PMT gain (see section 3), s the threshold setting of the discriminator (in ADC channel) and a (0.39 ns), b (2.5 ns) and c (15.8 ns*ADC channel) the parameters extracted from a fit of the time distributions after slewing correction (figure 5-right). The first term of this equation is related to the intrinsic resolution of the detector and the second term to the photo-electron statistics. The last term comes from the uncertainty of the slewing correction due to fluctuations of the collected charge (derivative of eq. (3.1)).

The weighted average time of flight of each array is then calculated as:

$$\langle T \rangle = \frac{\sum_{i=1}^{32} \omega_i(Q_i) \times T_i}{\sum_{i=1}^{32} \omega_i(Q_i)}, \tag{4.2}$$

2013 JINST 8 P10016

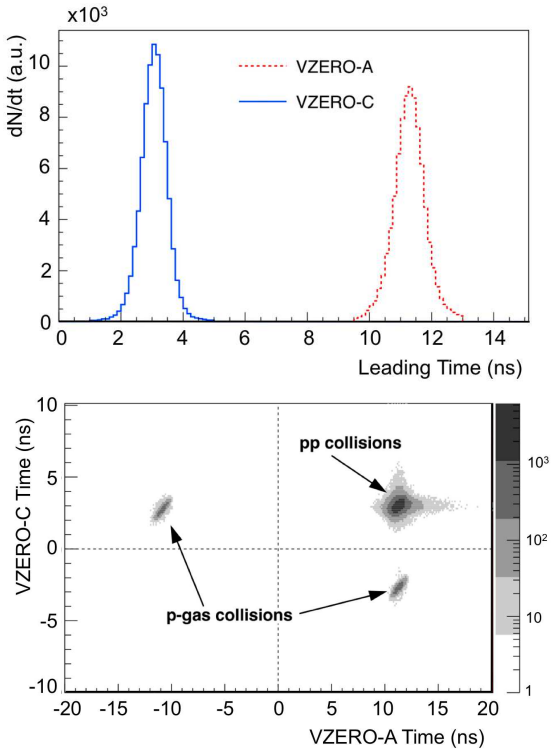

Figure 6. Top: VZERO-A (red-dashed line) and VZERO-C (blue-solid line) weighted average time of flight distributions for beam-beam collisions, with 0.45 and 0.35 ns r.m.s. respectively. Bottom: weighted average time of flight (as defined by eq. (4.2)) of the particles detected in VZERO-C versus VZERO-A. The dashed line intersection represents the time of the collisions at the interaction point, or the crossing time of the background tracks at the vertical plane $z = 0$.

where T_i and $\omega_i(Q_i)$ are respectively the leading time and the weight (calculated using eq. (4.1)) for channel i. One average time is calculated for each array, and the sum runs over all fired channels of the corresponding array. Time resolutions of about 450 ps and 350 ps are achieved for VZERO-A and VZERO-C arrays (figure 6-top).

Finally, the VZERO system allows rejection of events coming from beam-induced backgrounds, by requiring a positive time of flight for both arrays (figure 6-bottom).

5 Luminosity measurement

The measurement of the absolute value of a reference process cross-section allows the determination of an absolute normalization scale for other cross-section measurements in the experiment [12]. In ALICE, the on-line monitoring of the luminosity uses a time coincidence between the two VZERO arrays. The rate R of this coincidence is given by [13]

$$R = A \cdot \varepsilon \cdot \sigma \cdot \mathscr{L}. \tag{5.1}$$

where σ is the inelastic cross-section, A the acceptance, ε the efficiency and $\mathscr{L}$ the luminosity.

A measurement of the luminosity was carried out using the van der Meer scan method [14] which measures the size and the shape of the colliding beams by observing the counting rate R in a

2013 JINST 8 P10016

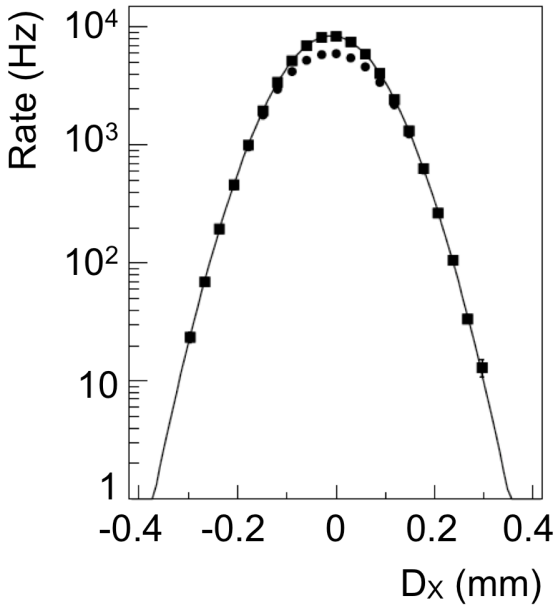

Figure 7. Example of $\mathrm{MB_{AND}}$ counting rate as a function of the beam displacement in the horizontal direction from the van der Meer scan data taken in May 2010 at an energy of 7 TeV in pp collisions. Dots represent the raw trigger rates and squares the interaction rates, and squares represents the interaction rates after corrections (see reference [15]). The line is used to guide the eye. The integral is calculated using the sum of all bins.

suitable monitor system while sweeping the two beams through each other. The rate corresponding to the coincidence between VZERO-A and VZERO-C signals is named $\mathrm{MB_{AND}}$. The luminosity $\mathscr{L}$ and therefore the rate of $\mathrm{MB_{AND}}(D_x, D_y)$ are functions of the transverse displacements D_x and D_y of the beams.

The shape factors Q_x and Q_y are obtained from the ratio of the area to the height of the rate curve in both directions (figure 7 for the x direction). For a zero degree crossing angle of beams with intensities N_1 and N_2 measured by the LHC [12], the luminosity $\mathscr{L}$, and hence the cross-section $\sigma_{\mathrm{MB_{AND}}}$ corresponding to the rate of $\mathrm{MB_{AND}}$, are obtained by:

$$\mathscr{L} = k_b f N_1 N_2 Q_x Q_y \quad \text{and} \quad \sigma_{\mathrm{MB_{AND}}} = \mathrm{MB_{AND}}(0,0)/\mathscr{L}, \tag{5.2}$$

where k_b is the number of colliding bunches and $f = 11.2455$ kHz the LHC revolution frequency.

The cross-section $\sigma_{\mathrm{MB_{AND}}}$ was measured for both pp colliding energies (2.76 TeV and 7 TeV) to be $\sigma_{\mathrm{MB_{AND}}}(2.76\ \mathrm{TeV}) = 47.7 \pm 0.9\ (\mathrm{syst.})$ mb and $\sigma_{\mathrm{MB_{AND}}}(7\ \mathrm{TeV}) = 54.3 \pm 1.9\ (\mathrm{syst.})$ mb. As a coincidence between VZERO-A and VZERO-C signals is required, this cross-section is not the minimum bias cross-section $\sigma_{\mathrm{MB_{OR}}}$. The triggering efficiency ($\sigma_{\mathrm{MB_{AND}}}/\sigma_{\mathrm{MB_{OR}}}$) was obtained from adjusted Monte Carlo simulations and evaluated to $(76.0\ ^{+5.2}_{-2.8})\%$ and $(74.2\ ^{+5.0}_{-2.0})\%$ respectively. A detailed description of this analysis can be found in reference [15]. This cross-section is then used between successive van der Meer scans to monitor the instantaneous luminosity using the $\mathrm{MB_{AND}}$ rate measurement. Hence, the VZERO system provides the integrated luminosity measurement for the ALICE experiment.

2013 JINST 8 P10016

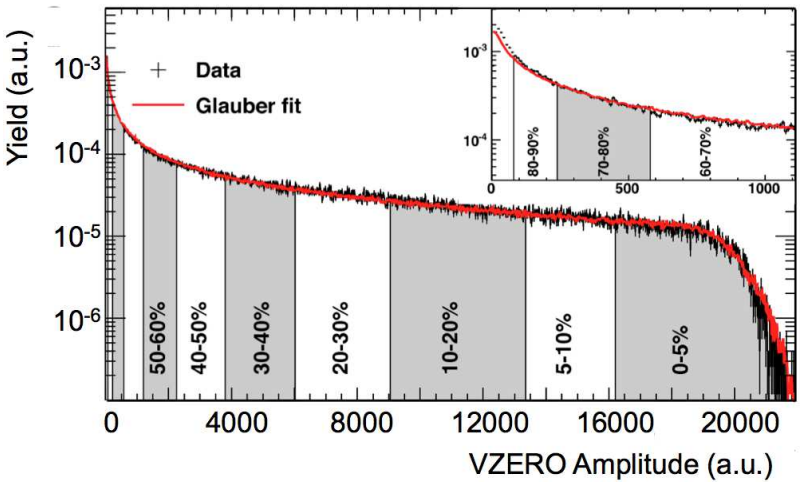

Figure 8. Distribution of the sum of amplitudes in the two VZERO arrays (black histogram) in Pb-Pb collisions at $\sqrt{s_{\rm NN}} = 2.76$ TeV [17]. The red line shows the fit with a Glauber model [19]. The shaded areas define the different centrality classes of hadronic collisions. The inset shows the low amplitude part of the distribution.

6 Multiplicity and centrality measurements

The VZERO system also provides a charged particle multiplicity measurement based on the energy deposited in the scintillators. Using a detailed simulation of the apparatus, the relation between the total charge collected inside a VZERO ring and the number of primary charged particles emitted into the corresponding pseudorapidity range was extracted. Therefore, it was possible to obtain the charged particle multiplicity, $\mathrm{d}N_{\rm ch}/\mathrm{d}\eta$, in eight pseudorapidity bins corresponding to the coverage of the different rings of the VZERO. This coverage was increased during the 2010 Pb-Pb run, for which satellite collisions at displaced vertices provided data [16–18]. These displaced vertices are found in the range $-187.5 < z < 375$ cm and were due to ions being captured in neighboring RF buckets during the beam injection procedure. The resulting effect is an increase of the η range covered by each array. In particular the η range seen by the VZERO-A array was extended to $-2.81 < \eta < 5.22$.

Figure 8 represents a typical distribution of the VZERO amplitudes [17]. The shaded areas correspond to the different centrality classes used in the physics analysis. The distribution is fit using a Glauber model [19] which reproduces correctly the VZERO amplitude distribution, hence the centrality, down to very low amplitudes (corresponding to peripheral events) where contribution from electromagnetic interactions between two lead ions is dominating (inset in figure 8). Figure 9 shows the centrality percentile resolution as a function of centrality for ZDC vs ZEM, TPC, SPD and VZERO systems [20]. The VZERO is used as the default in the ALICE experiment because it gives the best resolution over the inspected centrality range.

7 Event plane determination

Thanks to its granularity in the azimuthal direction (8 sectors of 45°, see figure 1), the VZERO system can be used to get an experimental estimate of the reaction plane, defined by the beam

2013 JINST 8 P10016

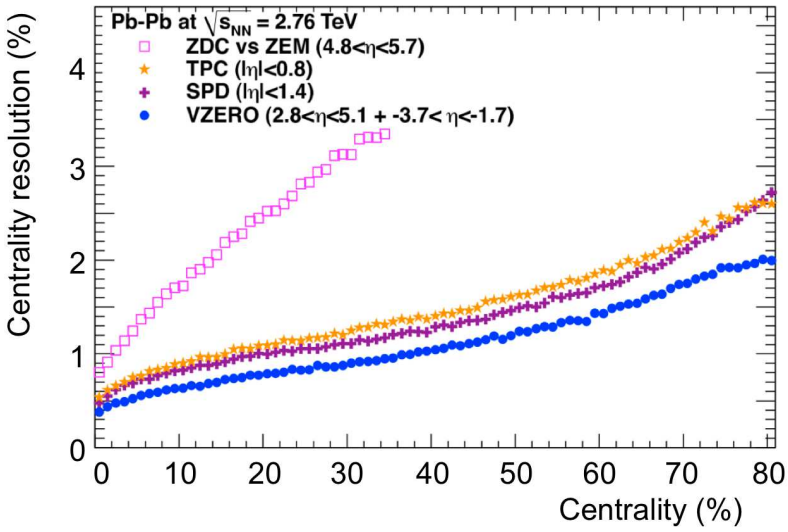

Figure 9. Centrality percentile resolution versus centrality for various ALICE detectors (see figure 3). This figure is extracted from [20].

direction and the line between the centers of the two nuclei along which the impact parameter is measured. The event plane is a key element in the study of the anisotropic particle flow which develops relatively to that plane and reflects properties of the system in the early stages of the collision. In practice, the anisotropic flow [21] is characterized with the help of a Fourier expansion of the Lorentz invariant azimuthal distribution of particles:

$$\rho(\phi - \Psi_{\mathrm{RP}}) = \frac{1}{2\pi}\left(1 + 2\sum_{n=1}^{\infty} v_n \cos[n(\phi - \Psi_{\mathrm{RP}})]\right), \tag{7.1}$$

where ϕ is the particle azimuthal angle, Ψ_{RP} the reaction plane angle as defined above and v_n the n-th harmonic of the anisotropic flow. Experimentally, due to interactions within the produced matter, the true reaction plane can only be reconstructed approximately. In practice, Ψ_{RP} has to be replaced in eq. (7.1) by the reconstructed "event plane" Ψ_n measured from the n-th harmonic anisotropy of the event itself. As a result, the observed flow coefficients v_n^{obs} have a magnitude smaller than the real flow coefficients v_n. Nevertheless, the true v_n can be approached by correcting the observed flow parameters v_n^{obs} knowing the event plane resolution $\mathscr{R}_{\Psi_n}$, i.e. the accuracy with which Ψ_n reproduces the true orientation of the reaction plane Ψ_{RP}: $v_n = v_n^{\mathrm{obs}}/\mathscr{R}_{\Psi_n}$.

The resolution can be extracted experimentally using a sub-event correlation technique [22]. Figure 10 shows the strong centrality dependence of the event plane resolution for the second harmonic. The event plane can be best determined for semi-central collisions where the flow effect is largest. The more isotropic the azimuthal event shape is, the more difficult is the extraction of the event plane and the poorer the resolution.

8 Conclusion

The VZERO is a detector system which plays a crucial role in ALICE. Over the first four years of operation at the LHC, the ALICE VZERO system showed an excellent operational efficiency, a

2013 JINST 8 P10016

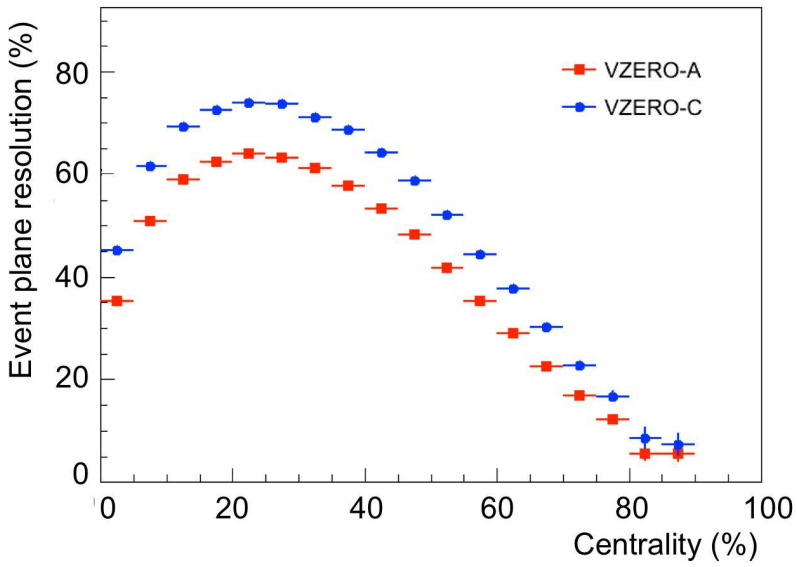

Figure 10. Second harmonic event plane resolution $\mathscr{R}_{\Psi_2}$ of VZERO-A and VZERO-C arrays as a function of centrality percentile.

necessary requirement for a system providing the lowest level triggers (L0) for the experiment. In addition, the VZERO system fulfills several important functions making use of its good time and charge resolution down to minimum ionizing particles. It is a powerful tool to reject beam-induced backgrounds and to measure and monitor the LHC luminosity. Moreover, it is also used to measure global properties of pp and Pb-Pb collisions such as particle multiplicity, collision centrality and event plane direction. The reduction of signal due to accumulated radiation doses was compensated, when necessary, by increasing the high voltage on each PMT. These adjustments have kept the detector fully operational without degrading its performance in time and charge resolution, except for some periods of high beam background during the 2012 run, when it was turned off as a conservation measure.

Acknowledgments

The ALICE collaboration would like to thank all its engineers and technicians for their invaluable contributions to the construction of the experiment and the CERN accelerator teams for the outstanding performance of the LHC complex.
The ALICE collaboration acknowledges the following funding agencies for their support in building and running the ALICE detector:
State Committee of Science, World Federation of Scientists (WFS) and Swiss Fonds Kidagan, Armenia,
Conselho Nacional de Desenvolvimento Científico e Tecnológico (CNPq), Financiadora de Estudos e Projetos (FINEP), Fundação de Amparo à Pesquisa do Estado de São Paulo (FAPESP);
National Natural Science Foundation of China (NSFC), the Chinese Ministry of Education (CMOE) and the Ministry of Science and Technology of China (MSTC);
Ministry of Education and Youth of the Czech Republic;

2013 JINST 8 P10016

Danish Natural Science Research Council, the Carlsberg Foundation and the Danish National Research Foundation;
The European Research Council under the European Community's Seventh Framework Programme;
Helsinki Institute of Physics and the Academy of Finland;
French CNRS-IN2P3, the 'Region Pays de Loire', 'Region Alsace', 'Region Auvergne' and CEA, France;
German BMBF and the Helmholtz Association;
General Secretariat for Research and Technology, Ministry of Development, Greece;
Hungarian OTKA and National Office for Research and Technology (NKTH);
Department of Atomic Energy and Department of Science and Technology of the Government of India;
Istituto Nazionale di Fisica Nucleare (INFN) and Centro Fermi - Museo Storico della Fisica e Centro Studi e Ricerche "Enrico Fermi", Italy;
MEXT Grant-in-Aid for Specially Promoted Research, Japan;
Joint Institute for Nuclear Research, Dubna;
(KICOS); National Research Foundation of Korea (NRF);
CONACYT, DGAPA, México, ALFA-EC and the EPLANET Program (European Particle Physics Latin American Network)
Stichting voor Fundamenteel Onderzoek der Materie (FOM) and the Nederlandse Organisatie voor Wetenschappelijk Onderzoek (NWO), Netherlands;
Research Council of Norway (NFR);
Polish Ministry of Science and Higher Education;
National Authority for Scientific Research - NASR (Autoritatea Naţională pentru Cercetare Ştiinţifică - ANCS);
Ministry of Education and Science of Russian Federation, Russian Academy of Sciences, Russian Federal Agency of Atomic Energy, Russian Federal Agency for Science and Innovations and The Russian Foundation for Basic Research;
Ministry of Education of Slovakia;
Department of Science and Technology, South Africa;
CIEMAT, EELA, Ministerio de Economía y Competitividad (MINECO) of Spain, Xunta de Galicia (Consellería de Educación), CEADEN, Cubaenergía, Cuba, and IAEA (International Atomic Energy Agency);
Swedish Research Council (VR) and Knut & Alice Wallenberg Foundation (KAW);
Ukraine Ministry of Education and Science;
United Kingdom Science and Technology Facilities Council (STFC);
The United States Department of Energy, the United States National Science Foundation, the State of Texas, and the State of Ohio.

References

[1] ALICE collaboration, *ALICE: Physics performance report, volume I*, *J. Phys.* **G 30** (2004) 1517.

[2] ALICE collaboration, *ALICE: Physics performance report, volume II*, *J. Phys.* **G 32** (2006) 1295.

2013 JINST 8 P10016

[3] ALICE collaboration, *ALICE forward detectors: FMD, TO and VO: Technical Design Report*, CERN-LHCC-2004-025 (2004).

[4] ALICE collaboration, *The ALICE experiment at the CERN LHC*, 2008 *JINST* **3** S08002.

[5] Saint Gobain Crystals, 104 route de Larchant BP 521, 77794 Nemours Cedex, France.

[6] Hamamatsu Photonics France, 19 rue du Saule Trapu, 91300 Massy, France; *Photomultiplier Tubes: Basics and Applications*, third edition (Edition 3A), 2007; *Photomultiplier Tubes and Related Products*, Feb. 2006 revised.

[7] Promic SAS, 46 rue de la Pierre Plantée, 42650 Saint Jean Bonnefonds, France.

[8] Y. Zoccarato et al., *Front end electronics and first results of the ALICE V0 detector*, *Nucl. Instrum. Meth.* **A626** (2011) 90.

[9] ALICE collaboration, *ALICE trigger data-acquisition high-level trigger and control system : Technical Design Report*, CERN-LHCC-2003-062 (2004).

[10] Photonis, Avenue Roger Roncier, BP 520, 19106 Brive Cedex, France.

[11] B. Cheynis et al., *Radiation effects on ALICE V0 detector components*, *Nucl. Instrum. Meth.* **A 569** (2006) 732.

[12] G. Anders et al., *LHC Bunch Current Normalisation for the April-May 2010 Luminosity Calibration Measurements*, CERN-ATS-Note-2011-004 (2011).

[13] K. Oyama, *Analysis of the May 2010 van der Meer scan in ALICE*, CERN-Proceedings-2011-001 (2011) 39.

[14] S. van der Meer, *Calibration of the effective beam height in the ISR*, ISR-PO/68-31, 18th June 1968.

[15] ALICE collaboration, *Measurement of inelastic, single- and double-diffraction cross sections in proton–proton collisions at the LHC with ALICE*, *Eur. Phys. J.* **C 73** (2013) 2456.

[16] ALICE collaboration, *Charged-particle multiplicity density at mid-rapidity in central Pb-Pb collisions at* $\sqrt{s_{NN}} = 2.76$ *TeV*, *Phys. Rev. Lett.* **105** (2010) 252301.

[17] ALICE collaboration, *Centrality dependence of the charged-particle multiplicity density at mid-rapidity in Pb-Pb collisions at* $\sqrt{s_{NN}} = 2.76$ *TeV*, *Phys. Rev. Lett.* **106** (2011) 032301.

[18] ALICE collaboration, *Centrality dependence of the pseudorapidity density distribution for charged particles in Pb-Pb collisions at* $\sqrt{s_{NN}} = 2.76$ *TeV*, CERN-PH-EP-2013-045, *Phys. Lett.* **B** (2013) in press.

[19] M.L. Miller, K. Reygers, S.J. Sanders and P. Steinberg, *Glauber modeling in high energy nuclear collisions*, *Ann. Rev. Nucl. Part. Sci.* **57** (2007) 205.

[20] ALICE collaboration, *Centrality determination of Pb-Pb collisions at* $\sqrt{s_{NN}} = 2.76$ *TeV with ALICE*, CERN-PH-EP-2012-368 (2012).

[21] I. Selyuzhenkov and S. Voloshin, *Effects of non-uniform acceptance in anisotropic flow measurement*, *Phys. Rev.* **C 77** (2008) 034904.

[22] A.M. Poskanzer and S. Voloshin, *Methods for analyzing anisotropic flow in relativistic nuclear collisions*, *Phys. Rev.* **C 58** (1998) 1671.

2013 JINST 8 P10016

The ALICE collaboration

E. Abbas[1], B. Abelev[72], J. Adam[38], D. Adamová[79], A.M. Adare[130], M.M. Aggarwal[83], G. Aglieri Rinella[34], M. Agnello[100,89], A.G. Agocs[129], A. Agostinelli[28], Z. Ahammed[124], N. Ahmad[18], A. Ahmad Masoodi[18], I. Ahmed[16], S.A. Ahn[65], S.U. Ahn[65], I. Aimo[25,100,89], M. Ajaz[16], A. Akindinov[51], D. Aleksandrov[95], B. Alessandro[100], D. Alexandre[97], R. Alfaro Molina[60], A. Alici[102,13], A. Alkin[4], E. Almaráz Aviña[61], J. Alme[36], T. Alt[40], V. Altini[32], S. Altinpinar[19], I. Altsybeev[126], C. Andrei[75], A. Andronic[92], V. Anguelov[88], J. Anielski[59], C. Anson[20], T. Antičić[93], F. Antinori[101], P. Antonioli[102], L. Aphecetche[108], H. Appelshäuser[57], N. Arbor[68], S. Arcelli[28], A. Arend[57], N. Armesto[17], R. Arnaldi[100], T. Aronsson[130], I.C. Arsene[92], M. Arslandok[57], A. Asryan[126], A. Augustinus[34], R. Averbeck[92], T.C. Awes[80], J. Äystö[43], M.D. Azmi[18,85], M. Bach[40], A. Badalà[99], Y.W. Baek[67,41], R. Bailhache[57], R. Bala[86,100], A. Baldisseri[15], F. Baltasar Dos Santos Pedrosa[34], J. Bán[52], R.C. Baral[53], R. Barbera[27], F. Barile[32], G.G. Barnaföldi[129], L.S. Barnby[97], V. Barret[67], J. Bartke[112], M. Basile[28], N. Bastid[67], S. Basu[124], B. Bathen[59], G. Batigne[108], B. Batyunya[63], P.C. Batzing[22], C. Baumann[57], I.G. Bearden[77], H. Beck[57], N.K. Behera[45], I. Belikov[62], F. Bellini[28], R. Bellwied[118], E. Belmont-Moreno[61], G. Bencedi[129], S. Beole[25], I. Berceanu[75], A. Bercuci[75], Y. Berdnikov[81], D. Berenyi[129], A.A.E. Bergognon[108], R.A. Bertens[50], D. Berzano[25,100], L. Betev[34], A. Bhasin[86], A.K. Bhati[83], J. Bhom[122], L. Bianchi[25], N. Bianchi[69], C. Bianchin[50], J. Bielčík[38], J. Bielčíková[79], A. Bilandzic[77], S. Bjelogrlic[50], F. Blanco[11], F. Blanco[118], D. Blau[95], C. Blume[57], M. Boccioli[34], S. Böttger[56], A. Bogdanov[73], H. Bøggild[77], M. Bogolyubsky[48], L. Boldizsár[129], M. Bombara[39], J. Book[57], H. Borel[15], A. Borissov[128], F. Bossú[85], M. Botje[78], E. Botta[25], E. Braidot[71], P. Braun-Munzinger[92], M. Bregant[108], T. Breitner[56], T.A. Broker[57], T.A. Browning[90], M. Broz[37], R. Brun[34], E. Bruna[25,100], G.E. Bruno[32], D. Budnikov[94], H. Buesching[57], S. Bufalino[25,100], P. Buncic[34], O. Busch[88], Z. Buthelezi[85], D. Caffarri[29,101], X. Cai[8], H. Caines[130], E. Calvo Villar[98], P. Camerini[23], V. Canoa Roman[12], G. Cara Romeo[102], W. Carena[34], F. Carena[34], N. Carlin Filho[115], F. Carminati[34], A. Casanova Díaz[69], J. Castillo Castellanos[15], J.F. Castillo Hernandez[92], E.A.R. Casula[24], V. Catanescu[75], C. Cavicchioli[34], C. Ceballos Sanchez[10], J. Cepila[38], P. Cerello[100], B. Chang[43,132], S. Chapeland[34], J.L. Charvet[15], S. Chattopadhyay[124], S. Chattopadhyay[96], M. Cherney[82], C. Cheshkov[34,117], B. Cheynis[117], V. Chibante Barroso[34], D.D. Chinellato[118], P. Chochula[34], M. Chojnacki[77], S. Choudhury[124], P. Christakoglou[78], C.H. Christensen[77], P. Christiansen[33], T. Chujo[122], S.U. Chung[91], C. Cicalo[103], L. Cifarelli[28,13], F. Cindolo[102], J. Cleymans[85], F. Colamaria[32], D. Colella[32], A. Collu[24], G. Conesa Balbastre[68], Z. Conesa del Valle[34,47], M.E. Connors[130], G. Contin[23], J.G. Contreras[12], T.M. Cormier[128], Y. Corrales Morales[25], P. Cortese[31], I. Cortés Maldonado[3], M.R. Cosentino[71], F. Costa[34], M.E. Cotallo[11], E. Crescio[12], P. Crochet[67], E. Cruz Alaniz[61], R. Cruz Albino[12], E. Cuautle[60], L. Cunqueiro[69], A. Dainese[29,101], R. Dang[8], A. Danu[55], K. Das[96], I. Das[47], S. Das[5], D. Das[96], S. Dash[45], A. Dash[116], S. De[124], G.O.V. de Barros[115], A. De Caro[30,13], G. de Cataldo[105], J. de Cuveland[40], A. De Falco[24], D. De Gruttola[30,13], H. Delagrange[i,108], A. Deloff[74], N. De Marco[100], E. Dénes[129], S. De Pasquale[30], A. Deppman[115], G. D Erasmo[32], R. de Rooij[50], M.A. Diaz Corchero[11], D. Di Bari[32], T. Dietel[59], C. Di Giglio[32], S. Di Liberto[106], A. Di Mauro[34], P. Di Nezza[69], R. Divià[34], Ø. Djuvsland[19], A. Dobrin[128,33,50], T. Dobrowolski[74], B. Dönigus[92,57], O. Dordic[22], A.K. Dubey[124], A. Dubla[50], L. Ducroux[117], P. Dupieux[67], A.K. Dutta Majumdar[96], D. Elia[105], D. Emschermann[59], H. Engel[56], B. Erazmus[34,108], H.A. Erdal[36], D. Eschweiler[40], B. Espagnon[47], M. Estienne[108], S. Esumi[122], D. Evans[97], S. Evdokimov[48], G. Eyyubova[22], D. Fabris[29,101], J. Faivre[68], D. Falchieri[28], A. Fantoni[69], M. Fasel[88], D. Fehlker[19], L. Feldkamp[59], D. Felea[55], A. Feliciello[100], B. Fenton-Olsen[71], G. Feofilov[126], A. Fernández Téllez[3], A. Ferretti[25], A. Festanti[29], J. Figiel[112], M.A.S. Figueredo[115], S. Filchagin[94], D. Finogeev[49], F.M. Fionda[32], E.M. Fiore[32], E. Floratos[84], M. Floris[34], S. Foertsch[85], P. Foka[92], S. Fokin[95], E. Fragiacomo[104], A. Francescon[34,29], U. Frankenfeld[92], U. Fuchs[34], C. Furget[68],

2013 JINST 8 P10016

M. Fusco Girard[30], J.J. Gaardhøje[77], M. Gagliardi[25], A. Gago[98], M. Gallio[25], D.R. Gangadharan[20], P. Ganoti[80], C. Garabatos[92], E. Garcia-Solis[14], C. Gargiulo[34], I. Garishvili[72], J. Gerhard[40], M. Germain[108], C. Geuna[15], M. Gheata[55,34], A. Gheata[34], B. Ghidini[32], P. Ghosh[124], P. Gianotti[69], P. Giubellino[34], E. Gladysz-Dziadus[112], P. Glässel[88], R. Gomez[114,12], E.G. Ferreiro[17], L.H. González-Trueba[61], P. González-Zamora[11], S. Gorbunov[40], A. Goswami[87], S. Gotovac[110], V. Grabski[60], L.K. Graczykowski[127], R. Grajcarek[88], A. Grelli[50], C. Grigoras[34], A. Grigoras[34], V. Grigoriev[73], A. Grigoryan[2], S. Grigoryan[63], B. Grinyov[4], N. Grion[104], P. Gros[33], J.F. Grosse-Oetringhaus[34], J.-Y. Grossiord[117], R. Grosso[34], F. Guber[49], R. Guernane[68], B. Guerzoni[28], M. Guilbaud[117], K. Gulbrandsen[77], H. Gulkanyan[2], T. Gunji[121], A. Gupta[86], R. Gupta[86], R. Haake[59], Ø. Haaland[19], C. Hadjidakis[47], M. Haiduc[55], H. Hamagaki[121], G. Hamar[129], B.H. Han[21], L.D. Hanratty[97], A. Hansen[77], Z. Harmanová-Tóthová[39], J.W. Harris[130], M. Hartig[57], A. Harton[14], D. Hatzifotiadou[102], S. Hayashi[121], A. Hayrapetyan[34,2], S.T. Heckel[57], M. Heide[59], H. Helstrup[36], A. Herghelegiu[75], G. Herrera Corral[12], N. Herrmann[88], B.A. Hess[123], K.F. Hetland[36], B. Hicks[130], B. Hippolyte[62], Y. Hori[121], P. Hristov[34], I. Hřivnáčová[47], M. Huang[19], T.J. Humanic[20], D.S. Hwang[21], R. Ichou[67], R. Ilkaev[94], I. Ilkiv[74], M. Inaba[122], E. Incani[24], G.M. Innocenti[25], P.G. Innocenti[34], M. Ippolitov[95], M. Irfan[18], C. Ivan[92], M. Ivanov[92], A. Ivanov[126], V. Ivanov[81], O. Ivanytskyi[4], A. Jachołkowski[27], P. M. Jacobs[71], C. Jahnke[115], H.J. Jang[65], M.A. Janik[127], P.H.S.Y. Jayarathna[118], S. Jena[45], D.M. Jha[128], R.T. Jimenez Bustamante[60], P.G. Jones[97], H. Jung[41], A. Jusko[97], A.B. Kaidalov[51], S. Kalcher[40], P. Kaliňák[52], T. Kalliokoski[43], A. Kalweit[34], J.H. Kang[132], V. Kaplin[73], S. Kar[124], A. Karasu Uysal[66], O. Karavichev[49], T. Karavicheva[49], E. Karpechev[49], A. Kazantsev[95], U. Kebschull[56], R. Keidel[133], B. Ketzer[57,111], M.M. Khan[18], P. Khan[96], S.A. Khan[124], K. H. Khan[16], A. Khanzadeev[81], Y. Kharlov[48], B. Kileng[36], M. Kim[132], T. Kim[132], B. Kim[132], S. Kim[21], M.Kim[41], D.J. Kim[43], J.S. Kim[41], J.H. Kim[21], D.W. Kim[41,65], S. Kirsch[40], I. Kisel[40], S. Kiselev[51], A. Kisiel[127], J.L. Klay[7], J. Klein[88], C. Klein-Bösing[59], M. Kliemant[57], A. Kluge[34], M.L. Knichel[92], A.G. Knospe[113], M.K. Köhler[92], T. Kollegger[40], A. Kolojvari[126], M. Kompaniets[126], V. Kondratiev[126], N. Kondratyeva[73], A. Konevskikh[49], V. Kovalenko[126], M. Kowalski[112], S. Kox[68], G. Koyithatta Meethaleveedu[45], J. Kral[43], I. Králik[52], F. Kramer[57], A. Kravčáková[39], M. Krelina[38], M. Kretz[40], M. Krivda[97,52], F. Krizek[43], M. Krus[38], E. Kryshen[81], M. Krzewicki[92], V. Kucera[79], Y. Kucheriaev[95], T. Kugathasan[34], C. Kuhn[62], P.G. Kuijer[78], I. Kulakov[57], J. Kumar[45], P. Kurashvili[74], A. Kurepin[49], A.B. Kurepin[49], A. Kuryakin[94], V. Kushpil[79], S. Kushpil[79], H. Kvaerno[22], M.J. Kweon[88], Y. Kwon[132], P. Ladrón de Guevara[60], C. Lagana Fernandes[115], I. Lakomov[47], R. Langoy[19,125], S.L. La Pointe[50], C. Lara[56], A. Lardeux[108], P. La Rocca[27], R. Lea[23], M. Lechman[34], S.C. Lee[41], G.R. Lee[97], I. Legrand[34], J. Lehnert[57], R.C. Lemmon[107], M. Lenhardt[92], V. Lenti[105], H. León[61], M. Leoncino[25], I. León Monzón[114], P. Lévai[129], S. Li[67,8], J. Lien[19,125], R. Lietava[97], S. Lindal[22], V. Lindenstruth[40], C. Lippmann[92,34], M.A. Lisa[20], H.M. Ljunggren[33], D.F. Lodato[50], P.I. Loenne[19], V.R. Loggins[128], V. Loginov[73], D. Lohner[88], C. Loizides[71], K.K. Loo[43], X. Lopez[67], E. López Torres[10], G. Løvhøiden[22], X.-G. Lu[88], P. Luettig[57], M. Lunardon[29], J. Luo[8], G. Luparello[50], C. Luzzi[34], R. Ma[130], K. Ma[8], D.M. Madagodahettige-Don[118], A. Maevskaya[49], M. Mager[58,34], D.P. Mahapatra[53], A. Maire[88], M. Malaev[81], I. Maldonado Cervantes[60], L. Malinina[63,ii], D. Mal'Kevich[51], P. Malzacher[92], A. Mamonov[94], L. Manceau[100], L. Mangotra[86], V. Manko[95], F. Manso[67], V. Manzari[105], Y. Mao[8], M. Marchisone[67,25], J. Mareš[54], G.V. Margagliotti[23,104], A. Margotti[102], A. Marín[92], C. Markert[113], M. Marquard[57], I. Martashvili[120], N.A. Martin[92], P. Martinengo[34], M.I. Martínez[3], G. Martínez García[108], Y. Martynov[4], A. Mas[108], S. Masciocchi[92], M. Masera[25], A. Masoni[103], L. Massacrier[108], A. Mastroserio[32], A. Matyja[112], C. Mayer[112], J. Mazer[120], R. Mazumder[46], M.A. Mazzoni[106], F. Meddi[26], A. Menchaca-Rocha[61], J. Mercado Pérez[88], M. Meres[37], Y. Miake[122], K. Mikhaylov[63,52,51], L. Milano[34,25], J. Milosevic[22,iii], A. Mischke[50], A.N. Mishra[87,46], D. Miśkowiec[92], C. Mitu[55], S. Mizuno[122], J. Mlynarz[128], B. Mohanty[124,76], L. Molnar[129,62], L. Montaño Zetina[12], M. Monteno[100], E. Montes[11], T. Moon[132], M. Morando[29],

2013 JINST 8 P10016

D.A. Moreira De Godoy[115], S. Moretto[29], A. Morreale[43], A. Morsch[34], V. Muccifora[69], E. Mudnic[110], S. Muhuri[124], M. Mukherjee[124], H. Müller[34], M.G. Munhoz[115], S. Murray[85], L. Musa[34], J. Musinsky[52], B.K. Nandi[45], R. Nania[102], E. Nappi[105], C. Nattrass[120], T.K. Nayak[124], S. Nazarenko[94], A. Nedosekin[51], M. Nicassio[32,92], M.Niculescu[55,34], B.S. Nielsen[77], T. Niida[122], S. Nikolaev[95], V. Nikolic[93], S. Nikulin[95], V. Nikulin[81], B.S. Nilsen[82], M.S. Nilsson[22], F. Noferini[102,13], P. Nomokonov[63], G. Nooren[50], A. Nyanin[95], A. Nyatha[45], C. Nygaard[77], J. Nystrand[19], A. Ochirov[126], H. Oeschler[58,34,88], S. Oh[130], S.K. Oh[41], J. Oleniacz[127], A.C. Oliveira Da Silva[115], J. Onderwaater[92], C. Oppedisano[100], A. Ortiz Velasquez[33,60], A. Oskarsson[33], P. Ostrowski[127], J. Otwinowski[92], K. Oyama[88], K. Ozawa[121], Y. Pachmayer[88], M. Pachr[38], F. Padilla[25], P. Pagano[30], G. Paić[60], F. Painke[40], C. Pajares[17], S.K. Pal[124], A. Palaha[97], A. Palmeri[99], V. Papikyan[2], G.S. Pappalardo[99], W.J. Park[92], A. Passfeld[59], D.I. Patalakha[48], V. Paticchio[105], B. Paul[96], A. Pavlinov[128], T. Pawlak[127], T. Peitzmann[50], H. Pereira Da Costa[15], E. Pereira De Oliveira Filho[115], D. Peresunko[95], C.E. Pérez Lara[78], D. Perrino[32], W. Peryt[127,i], A. Pesci[102], Y. Pestov[6], V. Petráček[38], M. Petran[38], M. Petris[75], P. Petrov[97], M. Petrovici[75], C. Petta[27], S. Piano[104], M. Pikna[37], P. Pillot[108], O. Pinazza[34], L. Pinsky[118], N. Pitz[57], D.B. Piyarathna[118], M. Planinic[93], M. Płoskoń[71], J. Pluta[127], T. Pocheptsov[63], S. Pochybova[129], P.L.M. Podesta-Lerma[114], M.G. Poghosyan[34], K. Polák[54], B. Polichtchouk[48], N. Poljak[50,93], A. Pop[75], S. Porteboeuf-Houssais[67], V. Pospíšil[38], B. Potukuchi[86], S.K. Prasad[128], R. Preghenella[102,13], F. Prino[100], C.A. Pruneau[128], I. Pshenichnov[49], G. Puddu[24], V. Punin[94], J. Putschke[128], H. Qvigstad[22], A. Rachevski[104], A. Rademakers[34], T.S. Räihä[43], J. Rak[43], A. Rakotozafindrabe[15], L. Ramello[31], S. Raniwala[87], R. Raniwala[87], S.S. Räsänen[43], B.T. Rascanu[57], D. Rathee[83], W. Rauch[34], A.W. Rauf[16], V. Razazi[24], K.F. Read[120], J.S. Real[68], K. Redlich[74,iv], R.J. Reed[130], A. Rehman[19], P. Reichelt[57], M. Reicher[50], F. Reidt[88], R. Renfordt[57], A.R. Reolon[69], A. Reshetin[49], F. Rettig[40], J.-P. Revol[34], K. Reygers[88], L. Riccati[100], R.A. Ricci[70], T. Richert[33], M. Richter[22], P. Riedler[34], W. Riegler[34], F. Riggi[27,99], A. Rivetti[100], M. Rodríguez Cahuantzi[3], A. Rodriguez Manso[78], K. Røed[19,22], E. Rogochaya[63], D. Rohr[40], D. Röhrich[19], R. Romita[92,107], F. Ronchetti[69], P. Rosnet[67], S. Rossegger[34], A. Rossi[34], P. Roy[96], C. Roy[62], A.J. Rubio Montero[11], R. Rui[23], R. Russo[25], E. Ryabinkin[95], A. Rybicki[112], S. Sadovsky[48], K. Šafařík[34], R. Sahoo[46], P.K. Sahu[53], J. Saini[124], H. Sakaguchi[44], S. Sakai[71], D. Sakata[122], C.A. Salgado[17], J. Salzwedel[20], S. Sambyal[86], V. Samsonov[81], X. Sanchez Castro[62], L. Šándor[52], A. Sandoval[61], M. Sano[122], G. Santagati[27], R. Santoro[34,13], J. Sarkamo[43], D. Sarkar[124], E. Scapparone[102], F. Scarlassara[29], R.P. Scharenberg[90], C. Schiaua[75], R. Schicker[88], H.R. Schmidt[123], C. Schmidt[92], S. Schuchmann[57], J. Schukraft[34], T. Schuster[130], Y. Schutz[34,108], K. Schwarz[92], K. Schweda[92], G. Scioli[28], E. Scomparin[100], R. Scott[120], P.A. Scott[97], G. Segato[29], I. Selyuzhenkov[92], S. Senyukov[62], J. Seo[91], S. Serci[24], E. Serradilla[11,61], A. Sevcenco[55], A. Shabetai[108], G. Shabratova[63], R. Shahoyan[34], S. Sharma[86], N. Sharma[120], S. Rohni[86], K. Shigaki[44], K. Shtejer[10], Y. Sibiriak[95], E. Sicking[59], S. Siddhanta[103], T. Siemiarczuk[74], D. Silvermyr[80], C. Silvestre[68], G. Simatovic[60,93], G. Simonetti[34], R. Singaraju[124], R. Singh[86], S. Singha[124,76], V. Singhal[124], T. Sinha[96], B.C. Sinha[124], B. Sitar[37], M. Sitta[31], T.B. Skaali[22], K. Skjerdal[19], R. Smakal[38], N. Smirnov[130], R.J.M. Snellings[50], C. Søgaard[33], R. Soltz[72], M. Song[132], J. Song[91], C. Soos[34], F. Soramel[29], I. Sputowska[112], M. Spyropoulou-Stassinaki[84], B.K. Srivastava[90], J. Stachel[88], I. Stan[55], G. Stefanek[74], M. Steinpreis[20], E. Stenlund[33], G. Steyn[85], J.H. Stiller[88], D. Stocco[108], M. Stolpovskiy[48], P. Strmen[37], A.A.P. Suaide[115], M.A. Subieta Vásquez[25], T. Sugitate[44], C. Suire[47], M. Suleymanov[16], R. Sultanov[51], M. Šumbera[79], T. Susa[93], T.J.M. Symons[71], A. Szanto de Toledo[115], I. Szarka[37], A. Szczepankiewicz[34], M. Szymański[127], J. Takahashi[116], M.A. Tangaro[32], J.D. Tapia Takaki[47], A. Tarantola Peloni[57], A. Tarazona Martinez[34], A. Tauro[34], G. Tejeda Muñoz[3], A. Telesca[34], A. Ter Minasyan[95], C. Terrevoli[32], J. Thäder[92], D. Thomas[50], R. Tieulent[117], A.R. Timmins[118], D. Tlusty[38], A. Toia[40,29,101], H. Torii[121], L. Toscano[100], V. Trubnikov[4], D. Truesdale[20], W.H. Trzaska[43], T. Tsuji[121], A. Tumkin[94], R. Turrisi[101], T.S. Tveter[22], J. Ulery[57], K. Ullaland[19], J. Ulrich[64,56], A. Uras[117], G.M. Urciuoli[106], G.L. Usai[24], M. Vajzer[38,79], M. Vala[63,52], L. Valencia Palomo[47], S. Vallero[25], P. Vande Vyvre[34], J.W. Van Hoorne[34],

2013 JINST 8 P10016

M. van Leeuwen[50], L. Vannucci[70], A. Vargas[3], R. Varma[45], M. Vasileiou[84], A. Vasiliev[95], V. Vechernin[126], M. Veldhoen[50], M. Venaruzzo[23], E. Vercellin[25], S. Vergara[3], R. Vernet[9], M. Verweij[50], L. Vickovic[110], G. Viesti[29], J. Viinikainen[43], Z. Vilakazi[85], O. Villalobos Baillie[97], Y. Vinogradov[94], L. Vinogradov[126], A. Vinogradov[95], T. Virgili[30], Y.P. Viyogi[124], A. Vodopyanov[63], M.A. Völkl[88], S. Voloshin[128], K. Voloshin[51], G. Volpe[34], B. von Haller[34], I. Vorobyev[126], D. Vranic[92,34], J. Vrláková[39], B. Vulpescu[67], A. Vyushin[94], V. Wagner[38], B. Wagner[19], R. Wan[8], Y. Wang[8], Y. Wang[88], M. Wang[8], K. Watanabe[122], M. Weber[118], J.P. Wessels[34,59], U. Westerhoff[59], J. Wiechula[123], J. Wikne[22], M. Wilde[59], G. Wilk[74], M.C.S. Williams[102], B. Windelband[88], M. Winn[88], C.G. Yaldo[128], Y. Yamaguchi[121], S. Yang[19], P. Yang[8], H. Yang[15,50], S. Yasnopolskiy[95], J. Yi[91], Z. Yin[8], I.-K. Yoo[91], J. Yoon[132], X. Yuan[8], I. Yushmanov[95], V. Zaccolo[77], C. Zach[38], C. Zampolli[102], S. Zaporozhets[63], A. Zarochentsev[126], P. Závada[54], N. Zaviyalov[94], H. Zbroszczyk[127], P. Zelnicek[56], I.S. Zgura[55], M. Zhalov[81], Y. Zhang[8], H. Zhang[8], X. Zhang[71,67,8], D. Zhou[8], Y. Zhou[50], F. Zhou[8], H. Zhu[8], J. Zhu[8], X. Zhu[8], J. Zhu[8], A. Zichichi[28,13], A. Zimmermann[88], G. Zinovjev[4], Y. Zoccarato[117], M. Zynovyev[4], M. Zyzak[57]

[i] *Deceased*
[ii] *Also at: M.V.Lomonosov Moscow State University, D.V.Skobeltsyn Institute of Nuclear Physics, Moscow, Russia*
[iii] *Also at: University of Belgrade, Faculty of Physics and "Vinča" Institute of Nuclear Sciences, Belgrade, Serbia*
[iv] *Also at: Institute of Theoretical Physics, University of Wroclaw, Wroclaw, Poland*

1 *Academy of Scientific Research and Technology (ASRT), Cairo, Egypt*
2 *A. I. Alikhanyan National Science Laboratory (Yerevan Physics Institute) Foundation, Yerevan, Armenia*
3 *Benemérita Universidad Autónoma de Puebla, Puebla, Mexico*
4 *Bogolyubov Institute for Theoretical Physics, Kiev, Ukraine*
5 *Bose Institute, Department of Physics and Centre for Astroparticle Physics and Space Science (CAPSS), Kolkata, India*
6 *Budker Institute for Nuclear Physics, Novosibirsk, Russia*
7 *California Polytechnic State University, San Luis Obispo, California, United States*
8 *Central China Normal University, Wuhan, China*
9 *Centre de Calcul de l'IN2P3, Villeurbanne, France*
10 *Centro de Aplicaciones Tecnológicas y Desarrollo Nuclear (CEADEN), Havana, Cuba*
11 *Centro de Investigaciones Energéticas Medioambientales y Tecnológicas (CIEMAT), Madrid, Spain*
12 *Centro de Investigación y de Estudios Avanzados (CINVESTAV), Mexico City and Mérida, Mexico*
13 *Centro Fermi - Museo Storico della Fisica e Centro Studi e Ricerche "Enrico Fermi", Rome, Italy*
14 *Chicago State University, Chicago, United States*
15 *Commissariat à l'Energie Atomique, IRFU, Saclay, France*
16 *COMSATS Institute of Information Technology (CIIT), Islamabad, Pakistan*
17 *Departamento de Física de Partículas and IGFAE, Universidad de Santiago de Compostela, Santiago de Compostela, Spain*
18 *Department of Physics Aligarh Muslim University, Aligarh, India*
19 *Department of Physics and Technology, University of Bergen, Bergen, Norway*
20 *Department of Physics, Ohio State University, Columbus, Ohio, United States*
21 *Department of Physics, Sejong University, Seoul, South Korea*
22 *Department of Physics, University of Oslo, Oslo, Norway*
23 *Dipartimento di Fisica dell'Università and Sezione INFN, Trieste, Italy*
24 *Dipartimento di Fisica dell'Università and Sezione INFN, Cagliari, Italy*
25 *Dipartimento di Fisica dell'Università and Sezione INFN, Turin, Italy*
26 *Dipartimento di Fisica dell'Università 'La Sapienza' and Sezione INFN, Rome, Italy*
27 *Dipartimento di Fisica e Astronomia dell'Università and Sezione INFN, Catania, Italy*
28 *Dipartimento di Fisica e Astronomia dell'Università and Sezione INFN, Bologna, Italy*

2013 JINST 8 P10016

[29] *Dipartimento di Fisica e Astronomia dell'Università and Sezione INFN, Padova, Italy*
[30] *Dipartimento di Fisica 'E.R. Caianiello' dell'Università and Gruppo Collegato INFN, Salerno, Italy*
[31] *Dipartimento di Scienze e Innovazione Tecnologica dell'Università del Piemonte Orientale and Gruppo Collegato INFN, Alessandria, Italy*
[32] *Dipartimento Interateneo di Fisica 'M. Merlin' and Sezione INFN, Bari, Italy*
[33] *Division of Experimental High Energy Physics, University of Lund, Lund, Sweden*
[34] *European Organization for Nuclear Research (CERN), Geneva, Switzerland*
[35] *Fachhochschule Köln, Köln, Germany*
[36] *Faculty of Engineering, Bergen University College, Bergen, Norway*
[37] *Faculty of Mathematics, Physics and Informatics, Comenius University, Bratislava, Slovakia*
[38] *Faculty of Nuclear Sciences and Physical Engineering, Czech Technical University in Prague, Prague, Czech Republic*
[39] *Faculty of Science, P.J. Šafárik University, Košice, Slovakia*
[40] *Frankfurt Institute for Advanced Studies, Johann Wolfgang Goethe-Universität Frankfurt, Frankfurt, Germany*
[41] *Gangneung-Wonju National University, Gangneung, South Korea*
[42] *Gauhati University, Department of Physics, Guwahati, India*
[43] *Helsinki Institute of Physics (HIP) and University of Jyväskylä, Jyväskylä, Finland*
[44] *Hiroshima University, Hiroshima, Japan*
[45] *Indian Institute of Technology Bombay (IIT), Mumbai, India*
[46] *Indian Institute of Technology Indore, Indore, India (IITI)*
[47] *Institut de Physique Nucléaire d'Orsay (IPNO), Université Paris-Sud, CNRS-IN2P3, Orsay, France*
[48] *Institute for High Energy Physics, Protvino, Russia*
[49] *Institute for Nuclear Research, Academy of Sciences, Moscow, Russia*
[50] *Nikhef, National Institute for Subatomic Physics and Institute for Subatomic Physics of Utrecht University, Utrecht, Netherlands*
[51] *Institute for Theoretical and Experimental Physics, Moscow, Russia*
[52] *Institute of Experimental Physics, Slovak Academy of Sciences, Košice, Slovakia*
[53] *Institute of Physics, Bhubaneswar, India*
[54] *Institute of Physics, Academy of Sciences of the Czech Republic, Prague, Czech Republic*
[55] *Institute of Space Sciences (ISS), Bucharest, Romania*
[56] *Institut für Informatik, Johann Wolfgang Goethe-Universität Frankfurt, Frankfurt, Germany*
[57] *Institut für Kernphysik, Johann Wolfgang Goethe-Universität Frankfurt, Frankfurt, Germany*
[58] *Institut für Kernphysik, Technische Universität Darmstadt, Darmstadt, Germany*
[59] *Institut für Kernphysik, Westfälische Wilhelms-Universität Münster, Münster, Germany*
[60] *Instituto de Ciencias Nucleares, Universidad Nacional Autónoma de México, Mexico City, Mexico*
[61] *Instituto de Física, Universidad Nacional Autónoma de México, Mexico City, Mexico*
[62] *Institut Pluridisciplinaire Hubert Curien (IPHC), Université de Strasbourg, CNRS-IN2P3, Strasbourg, France*
[63] *Joint Institute for Nuclear Research (JINR), Dubna, Russia*
[64] *Kirchhoff-Institut für Physik, Ruprecht-Karls-Universität Heidelberg, Heidelberg, Germany*
[65] *Korea Institute of Science and Technology Information, Daejeon, South Korea*
[66] *KTO Karatay University, Konya, Turkey*
[67] *Laboratoire de Physique Corpusculaire (LPC), Clermont Université, Université Blaise Pascal, CNRS–IN2P3, Clermont-Ferrand, France*
[68] *Laboratoire de Physique Subatomique et de Cosmologie (LPSC), Université Joseph Fourier, CNRS-IN2P3, Institut Polytechnique de Grenoble, Grenoble, France*
[69] *Laboratori Nazionali di Frascati, INFN, Frascati, Italy*
[70] *Laboratori Nazionali di Legnaro, INFN, Legnaro, Italy*
[71] *Lawrence Berkeley National Laboratory, Berkeley, California, United States*
[72] *Lawrence Livermore National Laboratory, Livermore, California, United States*
[73] *Moscow Engineering Physics Institute, Moscow, Russia*
[74] *National Centre for Nuclear Studies, Warsaw, Poland*
[75] *National Institute for Physics and Nuclear Engineering, Bucharest, Romania*

2013 JINST 8 P10016

[76] *National Institute of Science Education and Research, Bhubaneswar, India*
[77] *Niels Bohr Institute, University of Copenhagen, Copenhagen, Denmark*
[78] *Nikhef, National Institute for Subatomic Physics, Amsterdam, Netherlands*
[79] *Nuclear Physics Institute, Academy of Sciences of the Czech Republic, Řež u Prahy, Czech Republic*
[80] *Oak Ridge National Laboratory, Oak Ridge, Tennessee, United States*
[81] *Petersburg Nuclear Physics Institute, Gatchina, Russia*
[82] *Physics Department, Creighton University, Omaha, Nebraska, United States*
[83] *Physics Department, Panjab University, Chandigarh, India*
[84] *Physics Department, University of Athens, Athens, Greece*
[85] *Physics Department, University of Cape Town and iThemba LABS, National Research Foundation, Somerset West, South Africa*
[86] *Physics Department, University of Jammu, Jammu, India*
[87] *Physics Department, University of Rajasthan, Jaipur, India*
[88] *Physikalisches Institut, Ruprecht-Karls-Universität Heidelberg, Heidelberg, Germany*
[89] *Politecnico di Torino, Turin, Italy*
[90] *Purdue University, West Lafayette, Indiana, United States*
[91] *Pusan National University, Pusan, South Korea*
[92] *Research Division and ExtreMe Matter Institute EMMI, GSI Helmholtzzentrum für Schwerionenforschung, Darmstadt, Germany*
[93] *Rudjer Bošković Institute, Zagreb, Croatia*
[94] *Russian Federal Nuclear Center (VNIIEF), Sarov, Russia*
[95] *Russian Research Centre Kurchatov Institute, Moscow, Russia*
[96] *Saha Institute of Nuclear Physics, Kolkata, India*
[97] *School of Physics and Astronomy, University of Birmingham, Birmingham, United Kingdom*
[98] *Sección Física, Departamento de Ciencias, Pontificia Universidad Católica del Perú, Lima, Peru*
[99] *Sezione INFN, Catania, Italy*
[100] *Sezione INFN, Turin, Italy*
[101] *Sezione INFN, Padova, Italy*
[102] *Sezione INFN, Bologna, Italy*
[103] *Sezione INFN, Cagliari, Italy*
[104] *Sezione INFN, Trieste, Italy*
[105] *Sezione INFN, Bari, Italy*
[106] *Sezione INFN, Rome, Italy*
[107] *Nuclear Physics Group, STFC Daresbury Laboratory, Daresbury, United Kingdom*
[108] *SUBATECH, Ecole des Mines de Nantes, Université de Nantes, CNRS-IN2P3, Nantes, France*
[109] *Suranaree University of Technology, Nakhon Ratchasima, Thailand*
[110] *Technical University of Split FESB, Split, Croatia*
[111] *Technische Universität München, Munich, Germany*
[112] *The Henryk Niewodniczanski Institute of Nuclear Physics, Polish Academy of Sciences, Cracow, Poland*
[113] *The University of Texas at Austin, Physics Department, Austin, TX, United States*
[114] *Universidad Autónoma de Sinaloa, Culiacán, Mexico*
[115] *Universidade de São Paulo (USP), São Paulo, Brazil*
[116] *Universidade Estadual de Campinas (UNICAMP), Campinas, Brazil*
[117] *Université de Lyon, Université Lyon 1, CNRS/IN2P3, IPN-Lyon, Villeurbanne, France*
[118] *University of Houston, Houston, Texas, United States*
[119] *University of Technology and Austrian Academy of Sciences, Vienna, Austria*
[120] *University of Tennessee, Knoxville, Tennessee, United States*
[121] *University of Tokyo, Tokyo, Japan*
[122] *University of Tsukuba, Tsukuba, Japan*
[123] *Eberhard Karls Universität Tübingen, Tübingen, Germany*
[124] *Variable Energy Cyclotron Centre, Kolkata, India*
[125] *Vestfold University College, Tonsberg, Norway*

2013 JINST 8 P10016

[126] *V. Fock Institute for Physics, St. Petersburg State University, St. Petersburg, Russia*
[127] *Warsaw University of Technology, Warsaw, Poland*
[128] *Wayne State University, Detroit, Michigan, United States*
[129] *Wigner Research Centre for Physics, Hungarian Academy of Sciences, Budapest, Hungary*
[130] *Yale University, New Haven, Connecticut, United States*
[131] *Yildiz Technical University, Istanbul, Turkey*
[132] *Yonsei University, Seoul, South Korea*
[133] *Zentrum für Technologietransfer und Telekommunikation (ZTT), Fachhochschule Worms, Worms, Germany*

2013 JINST 8 P10016